Article

Current Biology

Metabolic evolution in response to interspecific competition in a eukaryote

Graphical abstract

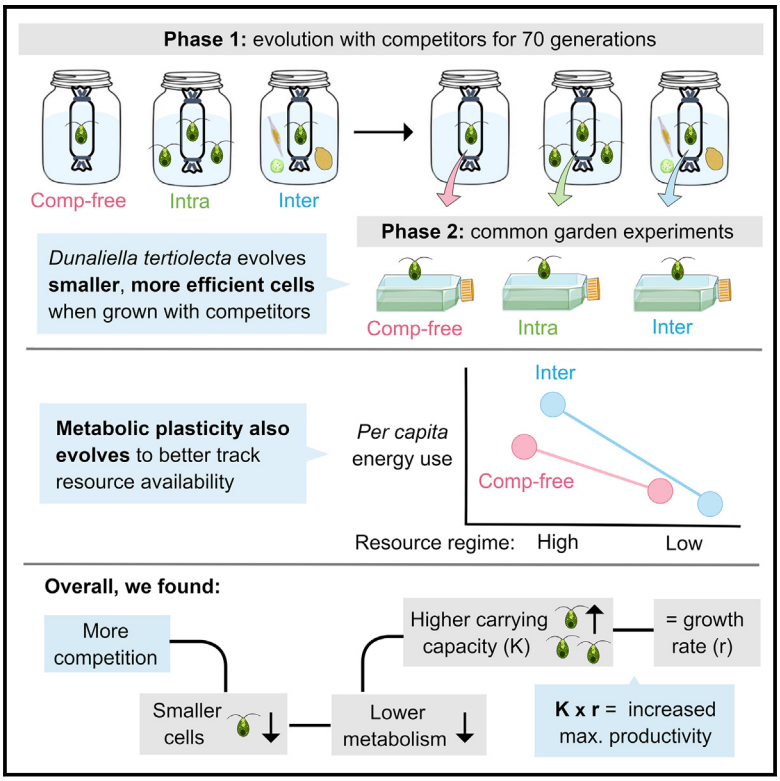

Highlights

- Competition selects for smaller and more energy-efficient microalgal cells
- Adaptive metabolic and size evolution maximize population carrying capacity
- Metabolic theory predicts most demographic changes
- Evolved metabolic plasticity reduces trade-offs between growth and carrying capacity

Authors

Giulia Ghedini, Dustin J. Marshall

Correspondence

gghedini@igc.gulbenkian.pt

In brief

Ghedini and Marshall show that the microalga *Dunaliella tertiolecta* evolves its size and metabolism in face of competition to increase efficiency in a way that is predicted by metabolic theory. But because metabolic plasticity evolves in parallel, competition-exposed populations maximize carrying capacity without reducing population growth rate.

Ghedini & Marshall, 2023, Current Biology *33*, 1–10
July 24, 2023
https://doi.org/10.1016/j.cub.2023.06.026

CellPress

Please cite this article in press as: Ghedini and Marshall, Metabolic evolution in response to interspecific competition in a eukaryote, Current Biology (2023), https://doi.org/10.1016/j.cub.2023.06.026

Current Biology

CellPress

Article

Metabolic evolution in response to interspecific competition in a eukaryote

Giulia Ghedini[1,2,3,5,*] and Dustin J. Marshall[1,4]
[1]Centre for Geometric Biology, School of Biological Sciences, Monash University, Clayton, VIC 3800, Australia
[2]Present address: Instituto Gulbenkian de Ciência, Rua Quinta Grande 6, 2780-156 Oeiras, Portugal
[3]Twitter: @giulia_ghedini
[4]Twitter: @djm_MEEG
[5]Lead contact
*Correspondence: gghedini@igc.gulbenkian.pt
https://doi.org/10.1016/j.cub.2023.06.026

SUMMARY

Competition drives rapid evolution, which, in turn, alters the trajectory of ecological communities. These eco-evolutionary dynamics are increasingly well-appreciated, but we lack a mechanistic framework for identifying the types of traits that will evolve and their trajectories. Metabolic theory offers explicit predictions for how competition should shape the (co)evolution of metabolism and size, but these are untested, particularly in eukaryotes. We use experimental evolution of a eukaryotic microalga to examine how metabolism, size, and demography coevolve under inter- and intraspecific competition. We find that the focal species evolves in accordance with the predictions of metabolic theory, reducing metabolic costs and maximizing population carrying capacity via changes in cell size. The smaller-evolved cells initially had lower population growth rates, as expected from their hyper-allometric metabolic scaling, but longer-term evolution yielded important departures from theory: we observed improvements in both population growth rate and carrying capacity. The evasion of this trade-off arose due to the rapid evolution of metabolic plasticity. Lineages exposed to competition evolved more labile metabolisms that tracked resource availability more effectively than lineages that were competition-free. That metabolic evolution can occur is unsurprising, but our finding that metabolic plasticity also co-evolves rapidly is new. Metabolic theory provides a powerful theoretical basis for predicting the eco-evolutionary responses to changing resource regimes driven by global change. Metabolic theory needs also to be updated to incorporate the effects of metabolic plasticity on the link between metabolism and demography, as this likely plays an underappreciated role in mediating eco-evolutionary dynamics of competition.

INTRODUCTION

When ecological and evolutionary processes occur on similar timescales, eco-evolutionary dynamics can shape the diversity and functioning of communities.[1–3] Studies in bacteria imply that competition within communities alters evolutionary trajectories in ways that are fundamentally different from simpler pairwise interactions.[4–7] Whether these results extend to eukaryotic communities, where species tend to have lower population densities and longer life cycles, and thus slower rates of evolution, remains unclear.[8] Macroevolutionary patterns in eukaryotes suggest that competition for resources can drive species to evolve differential resource use (e.g., Darwin's finches),[9–11] but such escapes from competition may not always be accessible.[12,13] In most cases, predicting trait evolution in species that share similar niches remains a formidable challenge.[8,14,15]

Life history theory provides general, qualitative predictions for how (intraspecific) competition should shape life history traits.[16] In a stable environment, competition should maximize population size (carrying capacity),[17] which is typically associated with more efficient phenotypes with a slower pace of life.[16,18] Populations that evolve under intense intraspecific competition indeed often show K-selected traits, including slower metabolisms (per unit mass) and reproduction,[18–20] but organisms with higher metabolisms can also be better competitors because they grow faster and can access more resources.[21–23] How organisms actually evolve when facing multiple, interspecific competitors remains unresolved.

Metabolic theory provides more quantitative predictions that should help with identifying the eco-evolutionary trajectories of key phenotypic traits in response to competition. The theory proposes that metabolism affects competition by setting per capita resource demands.[24,25] In particular, the scaling exponent "B" relating metabolic rate with body mass ($MR = aM^B$, where MR is metabolic rate and M is body mass) generates several quantitative predictions for how the size of organisms affects population parameters.[24,26] Because metabolism per unit mass fuels biological work, population growth rate should scale with body size at $B - 1$ ($r_{max} = M^B/M^1 = M^{B-1}$), if the cost of producing a new organism is proportional to size (though this is not always the case[27]). If metabolism scales at 0.75, as it does for many species, then population growth rate scales at −0.25 with body size.

Please cite this article in press as: Ghedini and Marshall, Metabolic evolution in response to interspecific competition in a eukaryote, Current Biology (2023), https://doi.org/10.1016/j.cub.2023.06.026

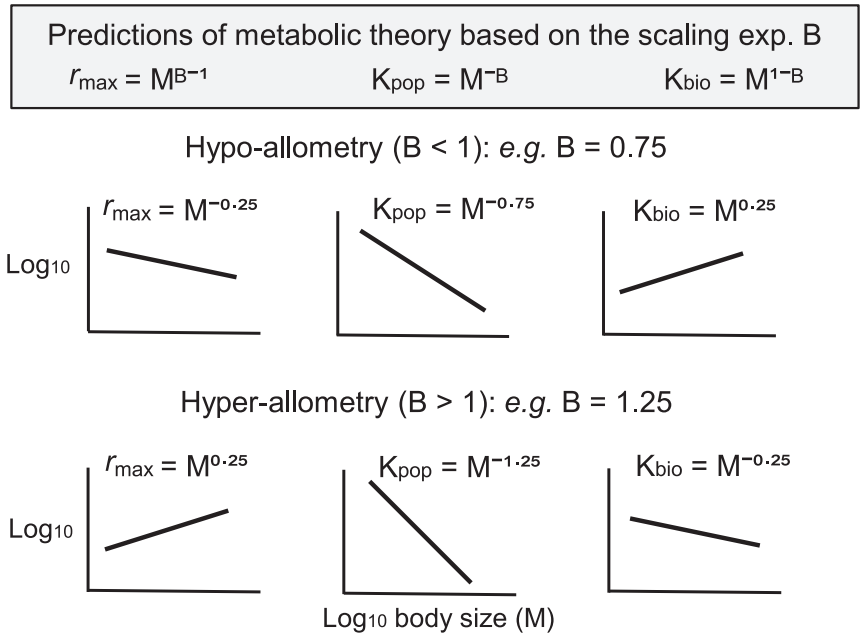

Figure 1. Demographic predictions of metabolic theory based on the scaling of metabolic rate (MR) with body size (M) on a log-log scale

The value B is the slope of the relationship between metabolism and size on a log-log scale. We provide examples for both hypo- (B < 1) and hyper-allometric (B > 1) metabolic scaling. In qualitative terms, if B is less than 1, metabolic theory predicts a negative relationship between population growth rate (r_{max}) and size, and between max. population density (K_{pop}) and size, while a positive relationship between max. total biomass (K_{bio}) and size. If B is greater than 1, then metabolic theory predicts a positive correlation between pop. growth rate and size, while a negative relationship between K_{pop} or K_{bio} and size.

A negative relationship between size and population growth is typical in interspecific comparisons: populations of mice grow more quickly than those of elephants.[25] It also follows that, if metabolism dictates resource requirements and populations are resource-limited, larger species should have lower population densities at carrying capacity than smaller species (K_{pop} should scale at $-B$) but greater total biomass because their mass-specific requirements are lower (K_{bio} scales at $1 - B$).[28] Of course, metabolism does not always scale with size at 0.75 and different metabolic scalings yield very different predictions.[29,30] We visualize the predictions of metabolic theory on population parameters for both cases of hypo- and hyper-allometric scaling (Figure 1), noting that demographic predictions can be calculated for any given value of B. Therefore, whatever the value of B, evolved changes in size and metabolism should affect both demography and capacity to compete with other species,[26,30] but whether size and metabolism coevolve in response to interspecific competition is untested.

We combined experimental evolution and metabolic theory to understand how size, metabolic fluxes, and demography coevolve in response to both intra- and interspecific competition in marine phytoplankton. We base our assessment on a focal species, the eukaryotic microalga *Dunaliella tertiolecta*, which we sourced as a non-clonal strain (CS-14) from the Australian National Algae Culture Collection. We evolved populations of this strain for ~70 generations in each of three environments: (1) competition-free, (2) intraspecific competition, and (3) interspecific competition (three other phytoplankton species). To manipulate the environment, we used dialysis bags that physically isolated the evolving population from its competitors, while exposing it to competition for light and nutrients[6,31–33] (Figure 2). We treated the competition-free lineages as a reference control. We batch-transferred both the focal species and the competitors weekly, standardizing biovolumes between treatments (~7 generations). We assessed how the focal populations had evolved at two points: at ~35 generations and ~70 generations. At each of these time points, we placed subsamples of all the evolved lineages of the focal species into a common environment and left them for several generations such that any persistent phenotypic differences that remained among treatments represented evolved responses to the environments.[34] We assessed changes in metabolism (photosynthesis, respiration, and net daily energy production), morphology (cell size and shape), and demography (growth rate, max. population density, and max. total biomass). We used the total biovolume of the population as a proxy for biomass, which we calculated as the product of cell size (μm^3) and population abundance (cells μL^{-1}). Common garden experiments lasted 16 days (until populations reached carrying capacity) and each lineage was phenotyped multiple times as populations grew (on 12 out of 16 days after 35 generations, and on 13 days after 70 generations). Finally, we tested how each demographic parameter scales with cell size in the evolved populations and compared these demographic observations with the predictions of metabolic theory. Because the scaling of metabolism with size can deviate from the classic assumption of 0.75,[29,30,35] we use the metabolic scaling exponents that we observed in our experiment.

RESULTS

Metabolism evolves under competition

After ~35 generations of experiencing interspecific competition, algae evolved lower metabolic fluxes than algae that experienced no interspecific competition. Specifically, rates of both photosynthesis and dark respiration were lower in lineages exposed to interspecific competition but only when we measured energy fluxes under resource limitation (photosynthesis, competition × biovolume interaction, $F_{2,\ 270} = 3.85$, $p = 0.02$; respiration, main competition effect, $F_{2,\ 272} = 6.56$, $p = 0.002$; Figure S1; Table S1). The lineages were the same when resources were abundant (Figure S1; Table S1). In other words, algae that experienced interspecific competition-evolved plasticity to have "thriftier" metabolisms when resources were scarce, reducing their rates of energy use—and presumably nutrient demand—while photosynthesizing, relative to other lineages.

Please cite this article in press as: Ghedini and Marshall, Metabolic evolution in response to interspecific competition in a eukaryote, Current Biology (2023), https://doi.org/10.1016/j.cub.2023.06.026

CellPress

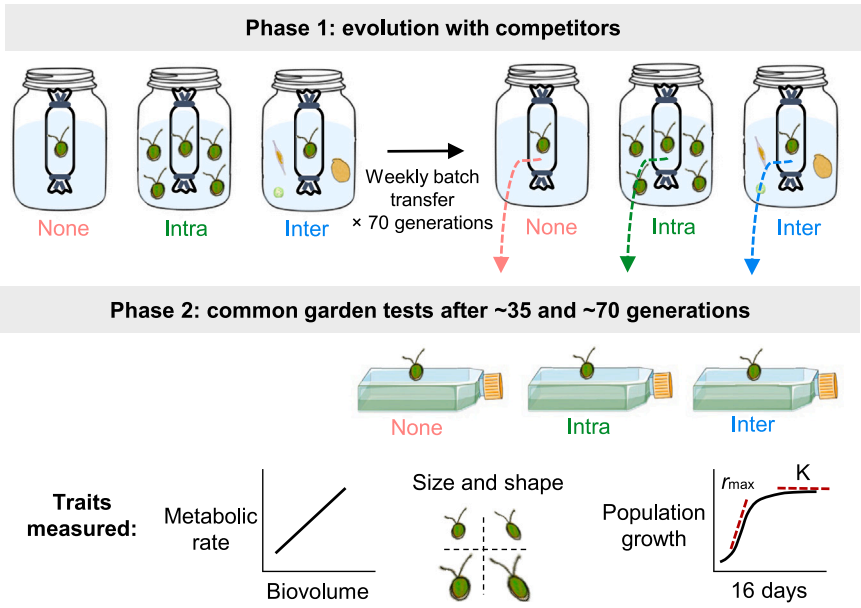

Figure 2. Experimental design

To test how metabolism, size, and demography coevolve in response to competition, we evolved the eukaryotic microalga *Dunaliella tertiolecta* in three environments: without competitors ("none") or with intraspecific ("intra") or interspecific competitors ("inter"). We enclosed the focal species in dialysis bags that physically isolated the evolving population from competitors while exposing it to competition for light and nutrients for 10 weeks, corresponding to approximately 70 generations. We propagated the focal lineages and the competitors performing weekly batch transfers. After ~35 and ~70 generations, we used common garden experiments to determine the evolved changes in metabolic fluxes, morphology, and demography between the focal populations.

After a further 35 generations of experimental evolution, interspecific competition drove more pronounced evolutionary changes in metabolism and metabolic plasticity. When we assessed metabolic fluxes under resource-limiting conditions, MRs (both photosynthesis and respiration) were lowest in lineages that had experienced interspecific competition and highest in those that experienced no competition (competition effect on photosynthesis, $F_{2,\ 47} = 6.75$, $p = 0.003$; Figure 3B; respiration, $F_{2,\ 47} = 15.83$, $p < 0.0001$; Figure 3D; Table S1). Again, lineages that evolved in the presence of competitors were thriftier when resources were scarce, particularly those that evolved with interspecifics. But when we assessed metabolic fluxes when resources were abundant, the patterns were reversed: lineages exposed to competition had greater rates of photosynthesis (competition × biovolume: $F_{2,\ 210} = 3.59$, $p = 0.03$; Figure 3A) and respiration (main competition effect: $F_{2,\ 46} = 10.86$, $p = 0.0001$; Figure 3C; Table S1) relative to competition-free lineages. Overall, competition-exposed lineages evolved more metabolic plasticity than competition-free lineages, downregulating their resource demands when resources were scarce and strongly upregulating their capacity to both fuel (via photosynthesis) and do (via respiration) biological work during periods of resource abundance (Figure 4, per capita rates; Figure S2, per unit-volume rates). In contrast, competition-free lineages exhibited more modest metabolic plasticity in response to changes in resource availability. Together, these evolved metabolic changes meant that competition-exposed lineages produced more energy on balance (photosynthesis − respiration), thereby fueling more biological work when resources were abundant (Figure 3E), but required fewer resources and produced less net energy when resource were scarce relative to competition-free lineages (Figure 3F).

Size co-evolves with metabolism

Lineages exposed to competition-evolved smaller cell sizes than lineages that were free from competition ($F_{2,\ 47} = 33.22$, $p < 0.0001$; Figure 5A for day 3 after 70 generations; estimated marginal means: competition-free = 202 [95% confidence interval (CI): 196, 207]; intra = 185 [179, 190]; inter = 162 [154, 170] μm^3). After 70 generations of experimental evolution, lineages experiencing interspecific competition were on average 13.4% smaller in cell volume than competition-free lineages (ranging from 3.6% to 19.6% smaller during common garden experiments), while those experiencing only intraspecific competition were intermediate in size (5.5% smaller on average; ranging from 0.6% larger to 8.5% smaller in size than competition-free lineages) (Figure S3 for all days of common garden; Table S2). Cell shape coevolved with size: cells exposed to competitors were rounder than cells from competition-free environments ($F_{2,\ 47} = 137.01$, $p < 0.0001$; Figure 5B for day 3; Figure S3 for all days; Table S3 for post hoc comparisons).

Metabolic scaling and predicting demography

While MRs often scale hypo-allometrically for eukaryotes, we found that both photosynthesis and respiration rates scaled hyper-allometrically with cell size in the focal populations (analyzing all competition treatments together, the scaling B is 1.31 [95% CI: 1.05; 1.58] for photosynthesis: and 1.28 [CI: 1.02; 1.55] for respiration; Table S4), similar to what was previously found for this species.[30] Thus, under hyper-allometry ($B > 1$), the smaller cells evolved under interspecific competition should have lower resource demands per capita in an absolute sense but also relative to cell biovolume. However, metabolic scaling became progressively shallower as populations grew denser over time (Table S4)—similar declines in metabolic scaling have been observed in phytoplankton under resource limitation.[36,37] Thus, because metabolic scaling changed with resource abundance, we calculated the demographic predictions of metabolic theory based on two scaling exponents B: the scaling observed during the exponential growth phase ($B_{exponential} = 1.13$), which should affect population growth rate (r_{max}), and the other scaling observed during the stationary phase ($B_{stationary} = 0.60$), which should affect carrying capacity K (both in terms of population abundance and biomass). Based on these scalings, metabolic theory would therefore make the following predictions regarding the scaling of demographic parameters with cell size[26,27,30]:

Please cite this article in press as: Ghedini and Marshall, Metabolic evolution in response to interspecific competition in a eukaryote, Current Biology (2023), https://doi.org/10.1016/j.cub.2023.06.026

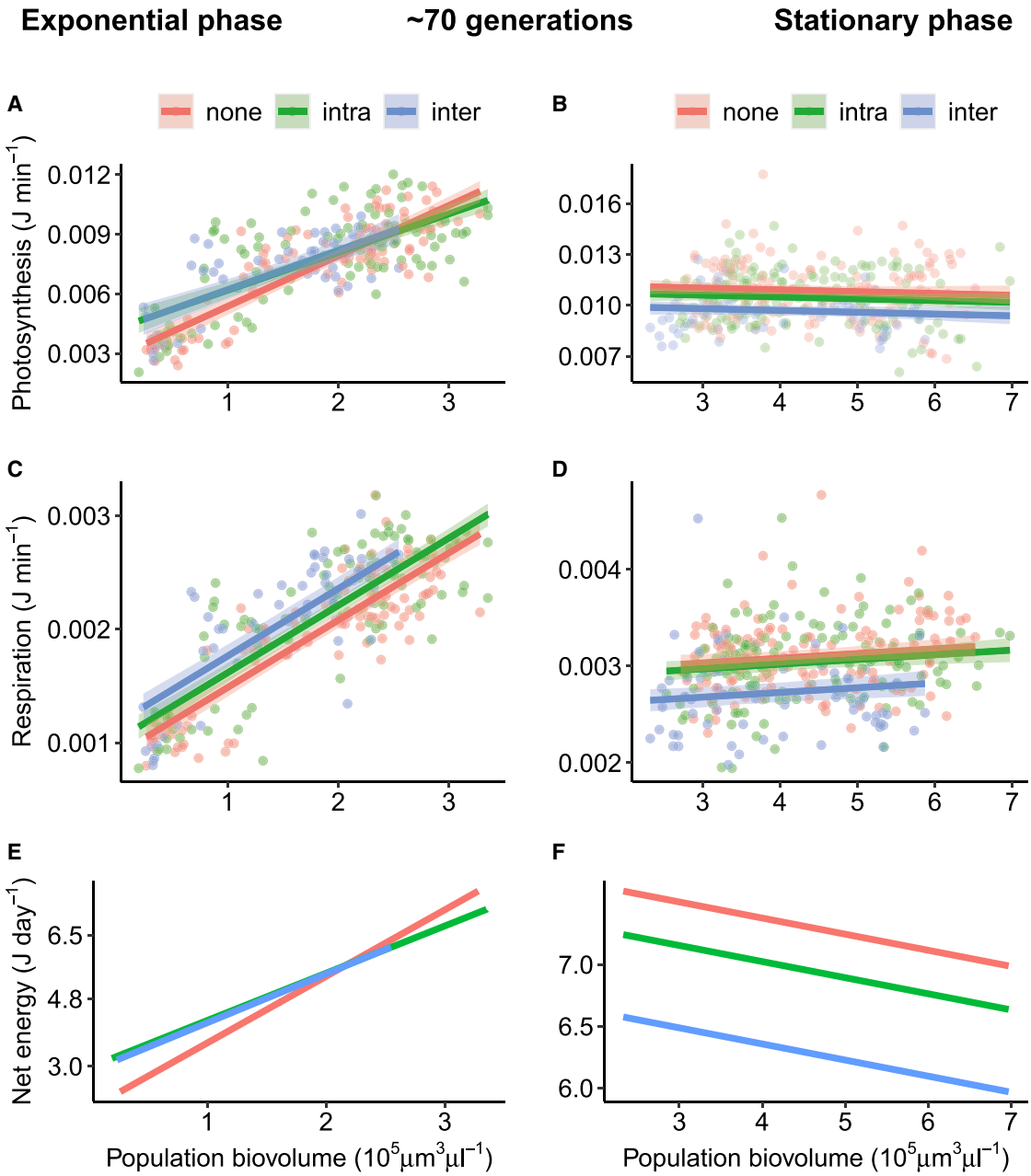

Figure 3. Populations exposed to competitors evolved faster metabolism during the exponential growth phase but lower metabolism during stationary phase

Here, we show evolution after ~70 generations for photosynthesis (A and B), respiration (C and D), and net energy (E and F), which is calculated as 14 h of photosynthesis minus 10 h of respiration. We tracked changes in population metabolism as biovolume grew during the common garden experiment, which lasted 16 days. We had 10 populations (lineages) from the interspecific competition treatment, 20 from the intraspecific treatment, and 20 competition-free; each of these populations was measured on 13 occasions (days). Thus, each data point represents the oxygen rate of a population on one of these days. Colored lines represent the best-fitting value and 95% confidence interval obtained from mixed models. See also Figure S1 for rates after 35 generations and Figure S5 and Table S1 for analyses.

$$r_{max} = M^{B\ exponential}/M^{1} = M^{0.13}, \quad \text{(Equation 1)}$$

$$K_{pop} = M^{0}/M^{B\ stationary} = M^{-0.60}, \quad \text{(Equation 2)}$$

$$K_{bio} = M \times K_{pop} = M \times M^{-B\ stationary} = M^{0.40}, \quad \text{(Equation 3)}$$

where B is the scaling exponent of MR with body size (M).

From these equations, we qualitatively predict that competition-exposed lineages (which evolved smaller body sizes) should

Please cite this article in press as: Ghedini and Marshall, Metabolic evolution in response to interspecific competition in a eukaryote, Current Biology (2023), https://doi.org/10.1016/j.cub.2023.06.026

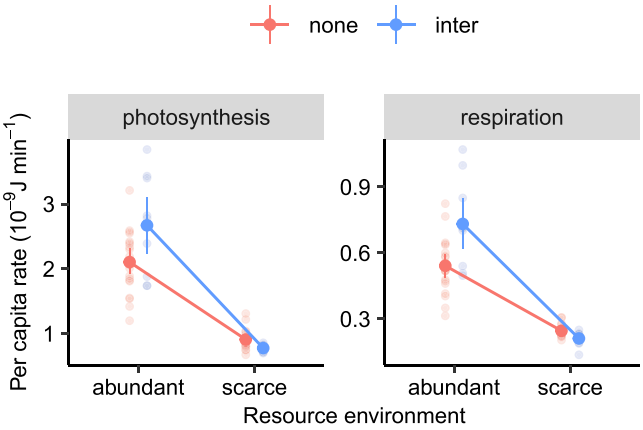

Figure 4. Populations exposed to interspecific competition for ~70 generations evolved greater metabolic plasticity relative to lineages that were competition-free

Cells with a history of competition (inter, n = 10) increase their metabolic rates (both photosynthesis and respiration) much more than control lineages (none, n = 20) when resources are abundant (day 3, exponential growth phase) but downregulate them when resources are scarce (day 11, stationary phase). This plasticity allows cells evolved with competitors to better track resource availability. Solid points represent the mean and bars the 95% bootstrapped confidence interval. See Figure S2 for per-unit biovolume rates.

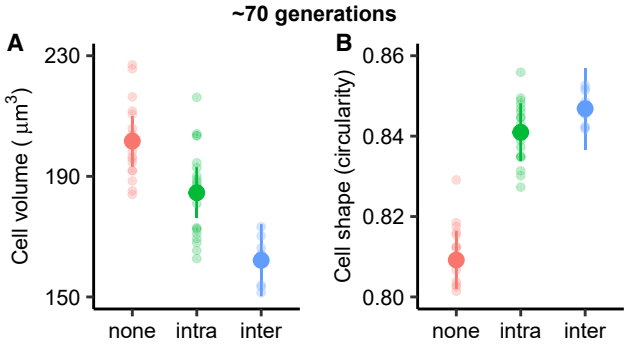

Figure 5. Both the cell size and shape of the microalga *Dunaliella tertiolecta* evolved in response to competition

(A) After ~70 generations, populations exposed to competitors evolved smaller cell sizes, with a stronger decline in response to interspecific than intraspecific competitors.

(B) Changes in cell size were accompanied by changes in shape: the smaller cells exposed to intra- and interspecific competitors were rounder than competition-free cells. This figure reports size and shape for day 3 of common garden experiments. Solid points and bars represent the least-squares means and 95% confidence level based on mixed models (n = 20 for "none" and "intra"; n = 10 for "inter").

See Figure S3 for the complete temporal series and Tables S2 and S3 for analyses.

have lower intrinsic rates of increase (r_{max}) but higher population carrying capacities (K_{pop}) than competition-free lineages. In a quantitative sense, we also predict that growth rate and biomass carrying capacity (K_{bio}) should positively covary with cell size, while population carrying capacity (K_{pop}) should negatively covary with cell size. We tested both sets of predictions experimentally.

The evolution of greater carrying capacity

We found strong qualitative and quantitative support for the demographic predictions based on metabolic theory. After ~35 generations, lineages that experienced competition had lower maximum growth rates (r_{max}) but greater carrying capacity (K_{pop}) than competition-free lineages (effect of competition on r_{max}, $F_{2,\ 42} = 10.46$, $p = 0.0002$; Figure 6A; effect on K_{pop}, $F_{2,\ 42} = 19.18$, $p < 0.0001$; Figure 6B). After 70 generations of experimental evolution, we found the same evolved difference in carrying capacity (K_{pop}; $F_{2,\ 46} = 13.91$, $p < 0.001$; Figure 6D), but the competition-exposed lineages had maximum population growth rates that were similar to the competition-free lineages ($F_{2,\ 46} = 1.97$, $p = 0.15$; Figure 6C; Table S5). Changes in demography were similar regardless of whether competition was intra- or interspecific (Figure S4; Table S5).

We compared our quantitative predictions derived from metabolic theory with the observed scaling of each demographic parameter with cell size for the focal populations and found remarkably strong congruence between the two for most parameters. We find that K_{pop} declines (cf.: observed = −0.56; predicted = −0.60; $F_{1,\ 48} = 22.4$, $p < 0.001$; 95% CI: −0.79; −0.32; Figure 7B) and K_{bio} increases with cell size, as predicted by theory (cf.: observed = 0.44; predicted = 0.40; $F_{1,\ 48} = 14.1$, $p < 0.001$; CI: 0.21; 0.68; Figure 7C). We find a weaker than predicted relationship between r_{max} and size (cf.: observed = 0.06; predicted = 0.13); this relationship is not significant as the CIs overlap zero ($F_{1,\ 48} = 0.02$, $p = 0.88$; CI: −0.71; 0.83; Figure 7A).

DISCUSSION

We found that intra- and interspecific competition drove the evolution of cell size and metabolism in the eukaryote *Dunaliella tertiolecta* in ways that metabolic theory anticipates. Because metabolism scaled hyper-allometrically with cell size in the focal lineages (when resources were not limiting), the evolution of smaller sizes in response to competition reduced per capita resource demands, both in absolute and relative terms. Accordingly, smaller cells achieved higher population densities. These increases in population carrying capacity initially came at the expense of population growth rates, as predicted by metabolic theory under hyper-allometric scaling (because smaller cells have lower rates of energy use per unit mass; Figure 1). However, through further evolution (~70 generations), competition-exposed lineages achieved improvements in both demographic traits: their max. population growth rates were comparable with those of competition-free lineages, while also maintaining higher population carrying capacities (Figure 7). The evolution of greater metabolic flexibility appeared to enable this change. Competition-exposed lineages were able to better downregulate their energy fluxes when resources were scare, but strongly upregulated their metabolism when resources were abundant, compared with competition-free lineages, thereby increasing both population growth rates and population carrying capacity. The evolution of enhanced metabolic plasticity is unanticipated by any theory base but, in hindsight, seems also inevitable. We eagerly await further studies that test the role of competition in driving

Please cite this article in press as: Ghedini and Marshall, Metabolic evolution in response to interspecific competition in a eukaryote, Current Biology (2023), https://doi.org/10.1016/j.cub.2023.06.026

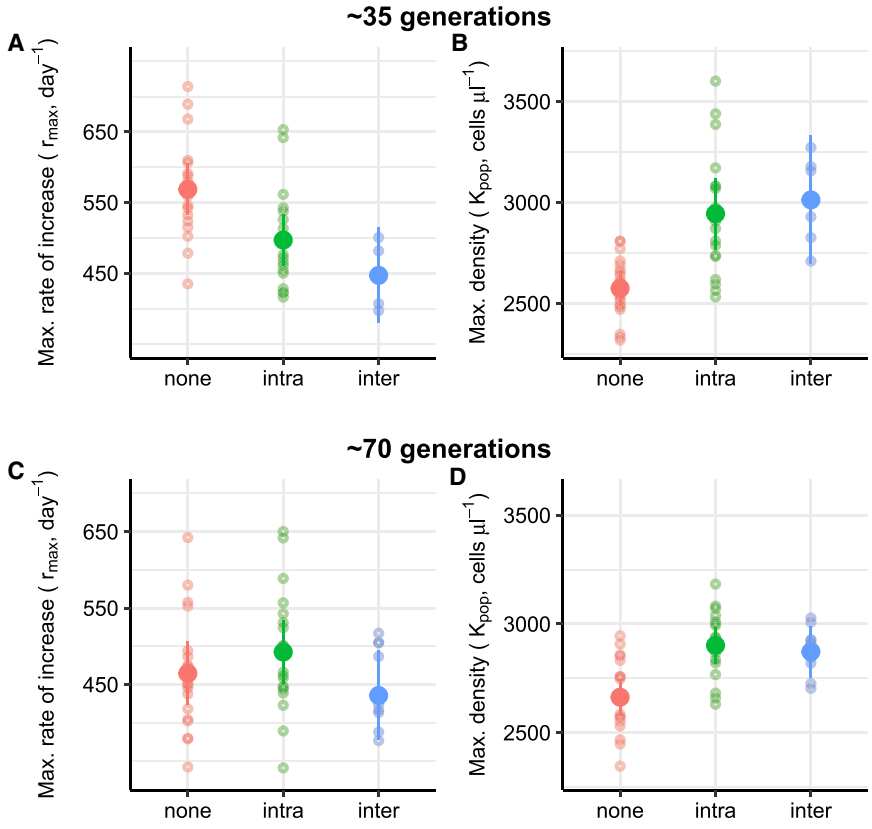

Figure 6. Lineages evolved with competitors had greater population carrying capacity (K_{pop})

(A and B) Initially (after 5 weeks of experimental evolution; ~35 generations), greater K_{pop} (B) came at the cost of maximum population growth rates (A).

(C and D) Differences in carrying capacity persisted after a further 35 generations (D) but with no differences in growth rates between competition environments (C). At either time, the type of competition experienced (intra- or interspecific) did not affect demographic parameters.

Solid points represent the mean growth parameters (r_{max} and K_{pop}, +95% confidence interval of the means) of each competition treatment (x axis): n = 20 for "none" and "intra"; n = 6 after 35 generations and n = 10 after 70 generations for "inter." The max. rate of population increase indicates the maximum value of the first derivative of the best-fitting growth model (r_{max}). Max. cell density (population size) indicates the maximum Y value in the best-fitting growth model (K_{pop}).

See also Figure S4 and Table S5 for analyses.

metabolic plasticity in other systems. For example, enhancements in plasticity might explain why within-species patterns do not always reflect the trade-offs observed among species.[14,38]

Metabolism sets resource demands and fuels growth; thus, MR should be under selection when competition is intense.[39] Life history (r-K selection) theory suggests that competition selects for efficiency, which is often associated with larger body sizes and lower mass-specific MRs, based on classic macroevolutionary patterns.[40–42] Metabolic theory offers more precise (quantitative) predictions for the evolution of size and metabolism, depending on the value of the scaling exponent B relating MR to body size. Our focal species exhibits hyper-allometric scaling of both photosynthesis (1.31) and respiration (1.28) with cell size; thus, while larger cells produce relatively more energy per capita, they are also both absolutely and relatively more expensive to maintain. Therefore, lineages exposed to competition-evolved smaller, more resource-efficient cells. Interestingly, long term experimental evolution (LTEE) in the prokaryote *Escherichia coli* yielded the opposite evolutionary trajectory of cell size to produce the same outcome—cells became larger over time to enhance resource-use efficiency.[27] Despite the different size trajectories, both studies conform with metabolic theory: in both, cells change size such that size-specific MRs decrease (metabolism scales hypo-allometrically with size in the LTEE, but hyper-allometrically in our study). Metabolic theory also successfully predicts the relationships between size, population density, and max. biomass in each study (based on species-specific metabolic scaling relationships). Based on our results, and those of Marshall et al.[27] and metabolic theory, we predict that competition should select for greater efficiency by favoring smaller body size in species with hyper-allometric metabolic scaling (B > 1) but larger body size in species with hypo-allometric scaling (B < 1). For metazoans, most species show hypo-allometric metabolic scaling within species (the appropriate biological scale in this instance), whereas intraspecific metabolic scaling in unicellular organisms remains largely unexplored, except for a few cases. We look forward to future studies that test how metabolic scaling and competition interact to determine the evolutionary trajectories of size, metabolism, and demography in other species, particularly other microbial species, given their pivotal role in driving biogeochemical cycles.[43,44]

Our findings have some concerning implications regarding global change. Phytoplankton play a key role in the global carbon budget, accounting for ~50% of all carbon fixed annually; thus, any change in phytoplankton productivity will strongly influence global carbon fluxes.[45] Ocean warming will intensify resource competition (because of increased water stratification) and decrease cell size within species.[46,47] Our competition-exposed lineages evolved smaller cells in response to stronger resource competition—in that sense, our experimental evolution mimics the impacts of global change. We found that the net energy fluxes of the competition-exposed lineages were ~15% lower in the stationary phase than those of competition-free lineages (Figure 3F). Hence, the net carbon assimilation rate and maximum total biomass of competition-evolved lineages were lower (Figure 7C). If natural phytoplankton populations also evolve smaller cell sizes in response to warming and/or nutrient limitation (and initial studies suggest that they do),[46] then our results would imply that rates of carbon assimilation and phytoplankton biomass will decline with further

Please cite this article in press as: Ghedini and Marshall, Metabolic evolution in response to interspecific competition in a eukaryote, Current Biology (2023), https://doi.org/10.1016/j.cub.2023.06.026

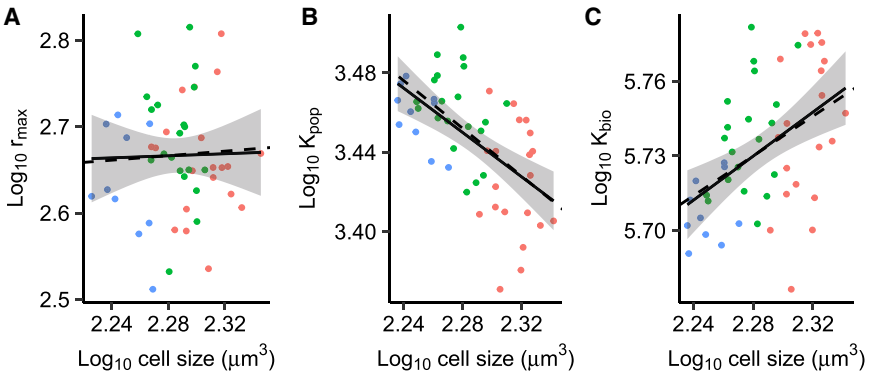

Figure 7. Scalings of population parameters with cell size after 70 generations of evolution

We find strong congruence between predictions from metabolic theory (broken lines) and demographic observations (solid lines). The scalings of max. growth rate (r_{max}), max. population density (K_{pop}), and max. biovolume (K_{bio}) with cell size are r_{max} = observed 0.06 (95% CI: −0.71; 0.83); predicted 0.13; K_{pop} = observed −0.56 (CI: −0.79; −0.32); predicted −0.60; K_{bio} = observed 0.44 (CI: 0.21; 0.68); predicted 0.40.

(A and B) In qualitative terms, lineages evolved with interspecific competitors had smaller cell sizes (blue) and reached greater max. population densities (B) while maintaining similar growth rates (A) than lineages evolved with intraspecific (green) or no competitors (red).

(C) But lineages evolved with competitors reached lower max. biomass.

Cell size differs between (A) and (B)/(C) because it is calculated for days 1–5 for r_{max} (because population growth is determined early on) and for days 12–16 for K_{pop} and K_{bio}, when cultures were in stationary phase. See STAR Methods for further details.

See also Figure S4 and Tables S4 and S5.

global change. While adaptation might dampen the negative effects of warming on phytoplankton productivity,[48,49] resource competition can increase the sensitivity of organisms to global change[7,50] and alter their evolution in ways that are poorly resolved.[4,6] Our results suggest that competition for resources might compound the impacts of global change by further selecting for smaller cell sizes and thriftier metabolisms that better tolerate competition but that may have undesirable impacts on carbon fixation.

Evolution happened rapidly in our system (within 70 generations). Such rapid evolution was likely fueled by the large population size of the founding non-clonal populations (~5 million cells). These rates of evolution are comparable to those observed in other experimental evolution studies of phytoplankton, where size and metabolic traits evolved within 100 generations,[49,51,52] whereas it takes longer for evolution to manifest when populations are derived from a single clone.[53] Genome sequencing would be necessary to determine whether the evolution we observed was driven by the differential reproduction of existing genotypes or the appearance and spread of new mutations. Overall, competition from a community exerted stronger effects on trait evolution than intraspecific competition, possibly because diverse competitors consume available resources more rapidly and effectively.[54,55] Thus, by posing a stronger selective pressure, competition from a community speeded up adaptation, countering the negative effects of reduced population sizes driven by resource competition,[56] similarly to what was observed in bacteria.[4,5] Still, we find remarkable consistency between the evolutionary responses to intra- and interspecific competition, with both selecting for smaller, more efficient cells able to sustain greater maximum population densities. This result accords with life history theory, which predicts that competition in stable or low stochastic environments should maximize carrying capacity (or equilibrium population size, K_{pop}).[16–18] Selection for r-K traits has been demonstrated in numerous systems within species,[18,39,57] but few studies have demonstrated the same principle in response to interspecific competition. MacArthur and Wilson first hypothesized in 1967 that selection for K should also apply in a community of species that compete for similar resources,[16] but, to our best knowledge, these results are a first experimental demonstration that this prediction also holds under interspecific competition. Given that evolution is predicted to maximize K and r,[58] and that these are strongly coupled to size and metabolism, we predict that changes in these demographic traits in response to competition are widespread.

Because size and metabolism together determine resource access and use,[46,59,60] changes in both traits might be a common feature of how species cope with shifts in competition and resource regimes. Both size and metabolic evolution might become more common, or rapid, as climate change, species introductions, and biodiversity loss alter competition for resources.[61,62] It seems likely that metabolic evolution will underpin many human-induced changes in resource regimes as well as mortality risks,[63] and we look forward to future studies that search for signatures of shifts in metabolism associated with changes in competition regimes.

STAR★METHODS

Detailed methods are provided in the online version of this paper and include the following:

- KEY RESOURCES TABLE
- RESOURCE AVAILABILITY
  - Lead contact
  - Materials availability
  - Data and code availability
- EXPERIMENTAL MODEL AND SUBJECT DETAILS
- METHOD DETAILS
  - Overview of experiments
  - Phase 1: evolution with competitors
  - Phase 2: common garden experiments
  - Morphology and population growth
  - Measuring metabolism
- QUANTIFICATION AND STATISTICAL ANALYSIS
  - Changes in morphology

- Changes in metabolism
- Changes in demography
- Testing predictions of metabolic theory

SUPPLEMENTAL INFORMATION

Supplemental information can be found online at https://doi.org/10.1016/j.cub.2023.06.026.

ACKNOWLEDGMENTS

We thank Mike McDonald, John DeLong, and Isabel Gordo for valuable comments on earlier versions of the manuscript. We also thank Jiaye Qin for assistance in data collection at Monash University and the Quantitative Biology Unit at the Instituto Gulbenkian de Ciência for statistical advice. This work was supported by the Australian Research Council through a DECRA fellowship (DE190100660) and by a fellowship (LCF/BQ/PI21/11830001) from "la Caixa" Foundation (ID 100010434) and the European Union's Horizon 2020 research and innovation programme under the Marie Skłodowska Curie grant agreement no. 847648 to G.G.

AUTHOR CONTRIBUTIONS

G.G. designed and performed the experiments. G.G. analyzed the data, with feedback from D.J.M., and produced the figures. G.G. wrote the first draft of the paper and both authors contributed substantially to revisions.

DECLARATION OF INTERESTS

The authors declare no competing interests.

INCLUSION AND DIVERSITY

We support inclusive, diverse, and equitable conduct of research.

Received: March 15, 2023
Revised: May 15, 2023
Accepted: June 8, 2023
Published: June 30, 2023

REFERENCES

1. Aubree, F., David, P., Jarne, P., Loreau, M., Mouquet, N., and Calcagno, V. (2020). How community adaptation affects biodiversity–ecosystem functioning relationships. Ecol. Lett. *23*, 1263–1275. https://doi.org/10.1111/ele.13530.
2. Post, D.M., and Palkovacs, E.P. (2009). Eco-evolutionary feedbacks in community and ecosystem ecology: interactions between the ecological theatre and the evolutionary play. Philos. Trans. R. Soc. Lond. B Biol. Sci. *364*, 1629–1640. https://doi.org/10.1098/rstb.2009.0012.
3. Hart, S.P., Turcotte, M.M., and Levine, J.M. (2019). Effects of rapid evolution on species coexistence. Proc. Natl. Acad. Sci. USA *116*, 2112–2117. https://doi.org/10.1073/pnas.1816298116.
4. Jousset, A., Eisenhauer, N., Merker, M., Mouquet, N., and Scheu, S. (2016). High functional diversity stimulates diversification in experimental microbial communities. Sci. Adv. *2*, e1600124, https://doi.org/10.1126/sciadv.1600124.
5. Lawrence, D., Fiegna, F., Behrends, V., Bundy, J.G., Phillimore, A.B., Bell, T., and Barraclough, T.G. (2012). Species interactions alter evolutionary responses to a novel environment. PLoS Biol. *10*, e1001330, https://doi.org/10.1371/journal.pbio.1001330.
6. Scheuerl, T., Hopkins, M., Nowell, R.W., Rivett, D.W., Barraclough, T.G., and Bell, T. (2020). Bacterial adaptation is constrained in complex communities. Nat. Commun. *11*, 754. https://doi.org/10.1038/s41467-020-14570-z.
7. García, F.C., Clegg, T., O'Neill, D.B., Warfield, R., Pawar, S., and Yvon-Durocher, G. (2023). The temperature dependence of microbial community respiration is amplified by changes in species interactions. Nat. Microbiol. *8*, 272–283. https://doi.org/10.1038/s41564-022-01283-w.
8. Barraclough, T.G. (2015). How do species interactions affect evolutionary dynamics across whole communities? Annu. Rev. Ecol. Evol. Syst. *46*, 25–48. https://doi.org/10.1146/annurev-ecolsys-112414-054030.
9. Grant, P.R., and Grant, B.R. (2006). Evolution of character displacement in Darwin's finches. Science *313*, 224–226. https://doi.org/10.1126/science.1128374.
10. Rainey, P.B., and Travisano, M. (1998). Adaptive radiation in a heterogeneous environment. Nature *394*, 69–72. https://doi.org/10.1038/27900.
11. Schluter, D. (1994). Experimental evidence that competition promotes divergence in adaptive radiation. Science *266*, 798–801. https://doi.org/10.1126/science.266.5186.798.
12. Abrams, P.A. (1987). Alternative models of character displacement and niche shift. I. Adaptive shifts in resource use when there is competition for nutritionally nonsubstitutable resources. Evolution *41*, 651–661. https://doi.org/10.1111/j.1558-5646.1987.tb05836.x.
13. Fox, J.W., and Vasseur, D.A. (2008). Character convergence under competition for nutritionally essential resources. Am. Nat. *172*, 667–680. https://doi.org/10.1086/591689.
14. Gallego, I., and Narwani, A. (2022). Ecology and evolution of competitive trait variation in natural phytoplankton communities under selection. Ecol. Lett. *25*, 2397–2409. https://doi.org/10.1111/ele.14103.
15. TerHorst, C.P., Zee, P.C., Heath, K.D., Miller, T.E., Pastore, A.I., Patel, S., Schreiber, S.J., Wade, M.J., and Walsh, M.R. (2018). Evolution in a community context: trait responses to multiple species interactions. Am. Nat. *191*, 368–380. https://doi.org/10.1086/695835.
16. MacArthur, R.H., and Wilson, E.O. (1967). The Theory of Island Biogeography (Princeton University Press).
17. Lande, R., Engen, S., and Saether, B.-E. (2009). An evolutionary maximum principle for density-dependent population dynamics in a fluctuating environment. Philos. Trans. R. Soc. Lond. B Biol. Sci. *364*, 1511–1518. https://doi.org/10.1098/rstb.2009.0017.
18. Sæther, B.E., Visser, M.E., Grøtan, V., and Engen, S. (2016). Evidence for r- and K-selection in a wild bird population: a reciprocal link between ecology and evolution. Proc. Biol. Sci. *283*, 20152411. https://doi.org/10.1098/rspb.2015.2411.
19. Auer, S.K., Dick, C.A., Metcalfe, N.B., and Reznick, D.N. (2018). Metabolic rate evolves rapidly and in parallel with the pace of life history. Nat. Commun. *9*, 14. https://doi.org/10.1038/s41467-017-02514-z.
20. Mueller, P., and Diamond, J. (2001). Metabolic rate and environmental productivity: well-provisioned animals evolved to run and idle fast. Proc. Natl. Acad. Sci. USA *98*, 12550–12554. https://doi.org/10.1073/pnas.221456698.
21. Schuster, L., Cameron, H., White, C.R., and Marshall, D.J. (2021). Metabolism drives demography in an experimental field test. Proc. Natl. Acad. Sci. USA *118*, e2104942118, https://doi.org/10.1073/pnas.2104942118.
22. Auer, S.K., Bassar, R.D., Turek, D., Anderson, G.J., McKelvey, S., Armstrong, J.D., Nislow, K.H., Downie, H.K., Morgan, T.A.J., McLennan, D., et al. (2020). Metabolic rate interacts with resource availability to determine individual variation in microhabitat use in the wild. Am. Nat. *196*, 132–144. https://doi.org/10.1086/709479.
23. Pettersen, A.K., Hall, M.D., White, C.R., and Marshall, D.J. (2020). Metabolic rate, context-dependent selection, and the competition-colonization trade-off. Evol. Lett. *4*, 333–344. https://doi.org/10.1002/evl3.174.
24. Brown, J.H., Gillooly, J.F., Allen, A.P., Savage, V.M., and West, G.B. (2004). Toward a metabolic theory of ecology. Ecology *85*, 1771–1789. https://doi.org/10.1890/03-9000.
25. Savage, V.M., Gillooly, J.F., Brown, J.H., West, G.B., and Charnov, E.L. (2004). Effects of body size and temperature on population growth. Am. Nat. *163*, 429–441. https://doi.org/10.1086/381872.

26. Isaac, N.J.B., Carbone, C., and McGill, B. (2012). Population and community ecology. In Metabolic Ecology, R.M. Sibly, J.H. Brown, and A. Kodric-Brown, eds. (Wiley-Blackwell).

27. Marshall, D.J., Malerba, M., Lines, T., Sezmis, A.L., Hasan, C.M., Lenski, R.E., and McDonald, M.J. (2022). Long-term experimental evolution decouples size and production costs in Escherichia coli. Proc. Natl. Acad. Sci. USA *119*, e2200713119, https://doi.org/10.1073/pnas.2200713119.

28. Damuth, J. (1981). Population-density and body size in mammals. Nature *290*, 699–700. https://doi.org/10.1038/290699a0.

29. Hatton, I.A., Dobson, A.P., Storch, D., Galbraith, E.D., and Loreau, M. (2019). Linking scaling laws across eukaryotes. Proc. Natl. Acad. Sci. USA *116*, 21616–21622. https://doi.org/10.1073/pnas.1900492116.

30. Malerba, M.E., and Marshall, D.J. (2019). Size-abundance rules? Evolution changes scaling relationships between size, metabolism and demography. Ecol. Lett. *22*, 1407–1416. https://doi.org/10.1111/ele.13326.

31. Berga, M., Székely, A.J., and Langenheder, S. (2012). Effects of disturbance intensity and frequency on bacterial community composition and function. PLoS One *7*, e36959, https://doi.org/10.1371/journal.pone.0036959.

32. Pomati, F., Jokela, J., Castiglioni, S., Thomas, M.K., and Nizzetto, L. (2017). Water-borne pharmaceuticals reduce phenotypic diversity and response capacity of natural phytoplankton communities. PLoS One *12*, e0174207, https://doi.org/10.1371/journal.pone.0174207.

33. Poulson-Ellestad, K.L., Jones, C.M., Roy, J., Viant, M.R., Fernández, F.M., Kubanek, J., and Nunn, B.L. (2014). Metabolomics and proteomics reveal impacts of chemically mediated competition on marine plankton. Proc. Natl. Acad. Sci. USA *111*, 9009–9014. https://doi.org/10.1073/pnas.1402130111.

34. de Villemereuil, P., Gaggiotti, O.E., Mouterde, M., and Till-Bottraud, I. (2016). Common garden experiments in the genomic era: new perspectives and opportunities. Heredity *116*, 249–254. https://doi.org/10.1038/hdy.2015.93.

35. Huete-Ortega, M., Cermeño, P., Calvo-Díaz, A., and Marañón, E. (2011). Isometric size-scaling of metabolic rate and the size abundance distribution of phytoplankton. Proc. R. Soc. Lond. B *279*, 1815–1823.

36. Finkel, Z.V., Irwin, A.J., and Schofield, O. (2004). Resource limitation alters the $^{3}/_{4}$ size scaling of metabolic rates in phytoplankton. Mar. Ecol. Prog. Ser. *273*, 269–279.

37. López-Sandoval, D.C., Rodríguez-Ramos, T., Cermeño, P., Sobrino, C., and Marañón, E. (2014). Photosynthesis and respiration in marine phytoplankton: relationship with cell size, taxonomic affiliation, and growth phase. J. Exp. Mar. Biol. Ecol. *457*, 151–159. https://doi.org/10.1016/j.jembe.2014.04.013.

38. Bernhardt, J.R., Kratina, P., Pereira, A.L., Tamminen, M., Thomas, M.K., and Narwani, A. (2020). The evolution of competitive ability for essential resources. Philos. Trans. R. Soc. Lond. B Biol. Sci. *375*, 20190247. https://doi.org/10.1098/rstb.2019.0247.

39. Bassar, R.D., Lopez-Sepulcre, A., Reznick, D.N., Travis, J., Brodie, A.E.E.D., and McPeek, E.M.A. (2013). Experimental evidence for density-dependent regulation and selection on Trinidadian guppy life histories. Am. Nat. *181*, 25–38. https://doi.org/10.1086/668590.

40. Pianka, E.R. (1970). On r- and K-selection. Am. Nat. *104*, 592–597.

41. Bierbaum, T.J., Mueller, L.D., and Ayala, F.J. (1989). Density-dependent evolution of life-history traits in Drosophila melanogaster. Evolution *43*, 382–392. https://doi.org/10.1111/j.1558-5646.1989.tb04234.x.

42. Mueller, L.D., and Ayala, F.J. (1981). Trade-off between r-selection and K-selection in Drosophila populations. Proc. Natl. Acad. Sci. USA *78*, 1303–1305. https://doi.org/10.1073/pnas.78.2.1303.

43. Gorter, F.A., Manhart, M., and Ackermann, M. (2020). Understanding the evolution of interspecies interactions in microbial communities. Philos. Trans. R. Soc. Lond. B Biol. Sci. *375*, 20190256. https://doi.org/10.1098/rstb.2019.0256.

44. Falkowski, P.G., Fenchel, T., and Delong, E.F. (2008). The microbial engines that drive earth's biogeochemical cycles. Science *320*, 1034–1039. https://doi.org/10.1126/science.1153213.

45. Field, C.B., Behrenfeld, M.J., Randerson, J.T., and Falkowski, P. (1998). Primary production of the biosphere: integrating terrestrial and oceanic components. Science *281*, 237–240. https://doi.org/10.1126/science.281.5374.237.

46. Hillebrand, H., Acevedo-Trejos, E., Moorthi, S.D., Ryabov, A., Striebel, M., Thomas, P.K., and Schneider, M.-L. (2022). Cell size as driver and sentinel of phytoplankton community structure and functioning. Funct. Ecol. *36*, 276–293. https://doi.org/10.1111/1365-2435.13986.

47. Yvon-Durocher, G., Montoya, J.M., Trimmer, M., and Woodward, G.U.Y. (2011). Warming alters the size spectrum and shifts the distribution of biomass in freshwater ecosystems. Glob. Change Biol. *17*, 1681–1694. https://doi.org/10.1111/j.1365-2486.2010.02321.x.

48. Barton, S., Jenkins, J., Buckling, A., Schaum, C.-E., Smirnoff, N., Raven, J.A., and Yvon-Durocher, G. (2020). Evolutionary temperature compensation of carbon fixation in marine phytoplankton. Ecol. Lett. *23*, 722–733. https://doi.org/10.1111/ele.13469.

49. Padfield, D., Yvon-Durocher, G., Buckling, A., Jennings, S., and Yvon-Durocher, G. (2016). Rapid evolution of metabolic traits explains thermal adaptation in phytoplankton. Ecol. Lett. *19*, 133–142. https://doi.org/10.1111/ele.12545.

50. Govaert, L., Gilarranz, L.J., and Altermatt, F. (2021). Competition alters species' plastic and genetic response to environmental change. Sci. Rep. *11*, 23518. https://doi.org/10.1038/s41598-021-02841-8.

51. Malerba, M.E., White, C.R., and Marshall, D.J. (2018). Eco-energetic consequences of evolutionary shifts in body size. Ecol. Lett. *21*, 54–62. https://doi.org/10.1111/ele.12870.

52. Bell, G. (2013). Experimental evolution of heterotrophy in a green alga. Evolution *67*, 468–476. https://doi.org/10.1111/j.1558-5646.2012.01782.x.

53. Collins, S. (2011). Competition limits adaptation and productivity in a photosynthetic alga at elevated CO_2. Proc. Biol. Sci. *278*, 247–255. https://doi.org/10.1098/rspb.2010.1173.

54. Maynard, D.S., Crowther, T.W., and Bradford, M.A. (2017). Competitive network determines the direction of the diversity–function relationship. Proc. Natl. Acad. Sci. USA *114*, 11464–11469. https://doi.org/10.1073/pnas.1712211114.

55. Vallina, S.M., Cermeno, P., Dutkiewicz, S., Loreau, M., and Montoya, J.M. (2017). Phytoplankton functional diversity increases ecosystem productivity and stability. Ecol. Modell. *361*, 184–196. https://doi.org/10.1016/j.ecolmodel.2017.06.020.

56. Osmond, M.M., and de Mazancourt, C. (2013). How competition affects evolutionary rescue. Philos. Trans. R. Soc. Lond. B Biol. Sci. *368*, 20120085. https://doi.org/10.1098/rstb.2012.0085.

57. Kentie, R., Clegg, S.M., Tuljapurkar, S., Gaillard, J.-M., and Coulson, T. (2020). Life-history strategy varies with the strength of competition in a food-limited ungulate population. Ecol. Lett. *23*, 811–820. https://doi.org/10.1111/ele.13470.

58. White, C.R., and Marshall, D.J. (2023). Optimisation and constraint: explaining metabolic patterns in biology. J. Exp. Biol. *226*, jeb245426.

59. Gallego, I., Venail, P., and Ibelings, B.W. (2019). Size differences predict niche and relative fitness differences between phytoplankton species but not their coexistence. ISME J. *13*, 1133–1143. https://doi.org/10.1038/s41396-018-0330-7.

60. Brandl, S.J., Quigley, C.N., Casey, J.M., Mercière, A., Schiettekatte, N.M.D., Norin, T., Parravicini, V., and Côté, I.M. (2022). Metabolic rates mirror morphological and behavioral differences in two sand-dwelling coral reef gobies. Mar. Ecol. Prog. Ser. *684*, 79–90. https://doi.org/10.3354/meps13968.

61. Alexander, J.M., Diez, J.M., and Levine, J.M. (2015). Novel competitors shape species' responses to climate change. Nature *525*, 515–518. https://doi.org/10.1038/nature14952.

62. Lancaster, L.T., Morrison, G., and Fitt, R.N. (2017). Life history trade-offs, the intensity of competition, and coexistence in novel and evolving communities under climate change. Philos. Trans. R. Soc. Lond. B Biol. Sci. *372*, 20160046. https://doi.org/10.1098/rstb.2016.0046.

63. White, C.R., Alton, L.A., Bywater, C.L., Lombardi, E.J., and Marshall, D.J. (2022). Metabolic scaling is the product of life-history optimization. Science *377*, 834–839. https://doi.org/10.1126/science.abm7649.

64. Schindelin, J., Arganda-Carreras, I., Frise, E., Kaynig, V., Longair, M., Pietzsch, T., Preibisch, S., Rueden, C., Saalfeld, S., Schmid, B., et al. (2012). Fiji: an open-source platform for biological-image analysis. Nat. Methods *9*, 676–682. https://doi.org/10.1038/nmeth.2019.

65. Pinheiro, J., and Bates, D. (2022). nlme: linear and nonlinear mixed effects models. R package version 3.1-161 (R core Team). https://CRAN.R-project.org/package=nlme.

66. Bates, D., Mächler, M., Bolker, B., and Walker, S. (2015). Fitting linear mixed-effects models using lme4. J. Stat. Soft. *67*, 48. https://doi.org/10.18637/jss.v067.i01.

67. Fox, J., and Weisberg, S. (2019). An {R} Companion to Applied Regression. Third Edition (Sage). https://socialsciences.mcmaster.ca/jfox/Books/Companion/.

68. Wickham, H. (2011). The split-apply-combine strategy for data analysis. J. Stat. Softw. *40*, 1–29. https://doi.org/10.18637/jss.v040.i01.

69. Wickham, H. (2016). ggplot2: Elegant Graphics for Data Analysis (Springer). https://ggplot2.tidyverse.org.

70. Wilke, C.O. (2016). Cowplot: Streamlined Plot Theme and Plot Annotations for 'ggplot2'. R Package Version 070. https://CRAN.R-project.org/package=cowplot.

71. Guillard, R.R.L., and Ryther, J.H. (1962). Studies of marine planktonic diatoms. I. *Cyclotella nana* Hustedt and *Detonula confervacea* Cleve. Can. J. Microbiol. *8*, 229–239.

72. Grant, N.A., Abdel Magid, A., Franklin, J., Dufour, Y., and Lenski, R.E. (2021). Changes in cell size and shape during 50,000 generations of experimental evolution with Escherichia coli. J. Bacteriol. *203*, e00469–e00420, https://doi.org/10.1128/JB.00469-20.

73. Ryabov, A., Kerimoglu, O., Litchman, E., Olenina, I., Roselli, L., Basset, A., Stanca, E., and Blasius, B. (2021). Shape matters: the relationship between cell geometry and diversity in phytoplankton. Ecol. Lett. *24*, 847–861. https://doi.org/10.1111/ele.13680.

74. Litchman, E., and Klausmeier, C.A. (2008). Trait-based community ecology of phytoplankton. Annu. Rev. Ecol. Evol. Syst. *39*, 615–639. https://doi.org/10.1146/annurev.ecolsys.39.110707.173549.

75. Tan, H., Hirst, A.G., Atkinson, D., and Kratina, P. (2021). Body size and shape responses to warming and resource competition. Funct. Ecol. *35*, 1460–1469. https://doi.org/10.1111/1365-2435.13789.

76. Hillebrand, H., Dürselen, C.-D., Kirschtel, D., Pollingher, U., and Zohary, T. (1999). Biovolume calculation for pelagic and benthic microalgae. J. Phycol. *35*, 403–424. https://doi.org/10.1046/j.1529-8817.1999.3520403.x.

77. Malerba, M.E., White, C.R., and Marshall, D.J. (2017). Phytoplankton size-scaling of net-energy flux across light and biomass gradients. Ecology *98*, 3106–3115. https://doi.org/10.1002/ecy.2032.

78. Ghedini, G., Marshall, D.J., and Loreau, M. (2022). Phytoplankton diversity affects biomass and energy production differently during community development. Funct. Ecol. *36*, 446–457.

79. Olito, C., White, C.R., Marshall, D.J., and Barneche, D.R. (2017). Estimating monotonic rates from biological data using local linear regression. J. Exp. Biol. *220*, 759–764.

80. White, C.R., Kearney, M.R., Matthews, P.G.D., Kooijman, S.A.L.M., and Marshall, D.J. (2011). A manipulative test of competing theories for metabolic scaling. Am. Nat. *178*, 746–754. https://doi.org/10.1086/662666.

81. Williams, P.J.l.B., and Laurens, L.M.L. (2010). Microalgae as biodiesel & biomass feedstocks: review & analysis of the biochemistry, energetics & economics. Energy Environ. Sci. *3*, 554–590. https://doi.org/10.1039/B924978H.

82. Malerba, M.E., Palacios, M.M., and Marshall, D.J. (2018). Do larger individuals cope with resource fluctuations better? An artificial selection approach. Proc. Biol. Sci. *285*, 20181347.

Please cite this article in press as: Ghedini and Marshall, Metabolic evolution in response to interspecific competition in a eukaryote, Current Biology (2023), https://doi.org/10.1016/j.cub.2023.06.026

STAR★METHODS

KEY RESOURCES TABLE

REAGENT or RESOURCE	SOURCE	IDENTIFIER
Biological samples		
Dunaliella tertiolecta	Australian National Algae Culture Collection (ANACC)	Strain ID: CS-14
Amphidinium carterae	ANACC	Strain ID: CS-740
Phaeodactylum tricornutum	ANACC	Strain ID: CS-29
Nannochloropsis oculata	ANACC	Strain ID: CS-179
Chemicals, peptides, and recombinant proteins		
Lugol solution	Sigma-Aldrich	Product no. L6146-1L
Sodium sulfite anhydrous	Sigma-Aldrich	SKU: 901916
Deposited data		
Data and code	Figshare	https://doi.org/10.26180/22137335
Experimental models: Organisms/strains		
Lineages of *Dunaliella tertiolecta* evolved competition-free, with intra- or inter-specific competitors	Centre for Geometric Biology, Monash University	N/A
Software and algorithms		
Fiji and ImageJ version 2.0	Schindelin et al.[64]	https://fiji.sc/
R Studio, Version 4.1.3	Team R	https://www.r-project.org/
nlme (R package)	Pinheiro and Bates[65]	CRAN mirror
lme4 (R package)	Bates et al.[66]	CRAN mirror
car (R package)	Fox and Weisberg[67]	CRAN mirror
plyr (R package)	Wickham[68]	CRAN mirror
ggplot2 (R package)	Wickham[69]	CRAN mirror
cowplot (R package)	Wilke[70]	CRAN mirror
Other		
PreSens Sensor Dish Readers & 5 mL vials	PreSens Precision Sensing	N/A
Olympus inverted microscope IX73	Olympus	N/A
Neubauer counting chamber	ProSciTech	N/A
Dialysis tubing, regenerated cellulose, 30m, 28mm diameter	Livingstone International	Product no. DTV12000.09.000

RESOURCE AVAILABILITY

Lead contact

Further information and requests for resources and data should be directed to the lead contact, Giulia Ghedini (gghedini@igc.gulbenkian.pt).

Materials availability

This study did not generate new or unique reagents or materials.

Data and code availability

- All data collected and analyzed in this paper have been deposited at Figshare and are publicly available as of the date of publication. DOI is listed in the key resources table. Microscopy data (photos) are available upon request to the corresponding author.
- All code used for analyses and figures has been deposited at Figshare and is publicly available as of the date of publication. DOI is listed in the key resources table.
- Any additional information required to reanalyze the data reported in this paper is available from the lead contact upon request.

Please cite this article in press as: Ghedini and Marshall, Metabolic evolution in response to interspecific competition in a eukaryote, Current Biology (2023), https://doi.org/10.1016/j.cub.2023.06.026

EXPERIMENTAL MODEL AND SUBJECT DETAILS

We sourced the eukaryotic microalga *Dunaliella tertiolecta* (Butcher) as a non-clonal strain from the Australian National Algae Culture Collection (ANACC; strain code CS-14). *Dunaliella* is a cosmopolitan, fast-growing green alga, which is mostly known to reproduce asexually (about 1 doubling per day). We used *Dunaliella* as the focal species of our study and sourced from ANACC three additional microalgal species that were used as interspecific competitors: *Amphidinium carterae* (CS-740), *Phaeodactylum tricornutum* (CS-29) and *Nannochloropsis oculata* (CS-179). These species are morphologically different so we could distinguish them *via* microscopy. Batch cultures of each species were maintained in 2 L glass bottles in a temperature-controlled room at 20 ± 1 °C using autoclaved f/2-Si media obtained from 0.45 μm-filtered seawater.[71] These cultures (one per species) were transferred to fresh media on a weekly basis for a month prior to the experiment. Light intensity was set at 115 ± 5 μmol photons m^{-2} s^{-1} with a photoperiod of 14-10 day-night cycle, using low-heat 50 W LED flood lights (Power-liteTM, Nedlands Group, Bedfordale, Australia). All experiments described below were done under the same growing conditions (light and temperature) and using the same type of media.

METHOD DETAILS

Overview of experiments

We tested the effects of intra- and inter-specific competition on the metabolism, morphology, and demography of the focal species *Dunaliella tertiolecta* (Figure 2). In a first phase, we experimentally evolved this species, enclosed in dialysis bags, in one of three environments for 10 weeks (~70 generations): 1) alone surrounded by media with no competitors (competition-free), 2) surrounded by a population of conspecifics from the same strain (intraspecific competition) or 3) by a community of three other microalgal species (interspecific competition using the species mentioned above: *Amphidinium*, *Phaeodactylum*, *Nannochloropsis*). In a second phase, we used common garden experiments to test how the traits of the focal species evolved in these different environments. We did this test twice: after 5 and 10 weeks of experimental evolution, approximately after 35 and 70 generations, respectively.

We started phase 1 (experimental evolution) with 20 lineages for each competition treatment but lost 13 lineages of the interspecific treatment because of contamination by *Phaeodactylum* in the first 6 weeks. To continue the experiment, we established an additional lineage from each of the remaining seven replicates but lost another 4 for the same reason by the end of the experiment. Thus, the data collected during common garden tests are from 6 lineages evolved with interspecific competitors after 35 generations (the seventh lineage was found contaminated during the common garden and thus discarded), and 10 lineages after 70 generations (n = 20 for the competition-free and intraspecific treatment). Common garden experiments lasted 16 days and all lineages were phenotyped multiple times as populations grew: once per day for 12 and 13 days after 35 and 70 generations, respectively.

Phase 1: evolution with competitors

The dialysis bags in which we enclosed the focal species enabled competition for light and nutrients but prevented cell mixing between species and exchange of bacteria (MWCO 12-14000 Da, pore size 24 Angstrom). Each bag was filled to a volume of 35 ml and was placed at the centre of a 500 ml glass jar assigned to one of the three competition treatments above.

We started the experiment with an initial biovolume (a proxy for biomass, obtained as cell volume × cell abundance) of 9.6×10^8 μm^3 of the focal species which corresponded 5×10^6 cells. This large initial population size meant that the founding populations likely contained a large amount of standing genetic variation. The glass jars containing the competitors were filled to 350 ml to completely submerge the dialysis bag. To maintain the same biovolume to media ratio, the initial biovolume of the competitors was 10 times that of the focal species (9.6×10^9 μm^3). We added the three competitor species of the interspecific treatment in equal biovolumes. The jars of the control treatment (competition-free) were filled with media only.

Each week we transferred a quantity equal to the initial biovolume (for both the focal species and the competitors) to a new, sterilized set of dialysis bags and jars. The batch-transfer approach meant that all populations in our experiment experienced fluctuating densities, but those surrounded by competitors always faced greater biomass densities and competition. We did not manipulate the relative abundance of species in the interspecific treatment during the experiment. In weeks 3, 5 and 6 the cell densities of the focal species were very low in the interspecific treatment – had we reinoculated the same initial biovolume we would not have been able to add fresh medium. To avoid this nutrient limitation, we reinoculated only half of the initial biovolumes across all treatments in these three occasions.

Phase 2: common garden experiments

After 5 and 10 weeks of experimental evolution (~35 and 70 generations, respectively), we tested all evolved lineages of the focal species for changes in morphology, metabolism, and demography. Before each common garden, we grew the focal species in a neutral environment (i.e. in cell culture flasks without competitors) for two generations to reduce any environmental conditioning (neutral selection). We then inoculated an equal biovolume of each lineage (~1.4×10^9 μm^3) in a 250 ml culture flask filled with media to 100 ml (n = 20 for the competition-free and intraspecific treatments, n = 6 and n = 10 for the interspecific treatment after 35 and 70 generations, respectively).

The common garden experiments lasted 16 days, which was the time needed for the cultures to reach carrying capacity. Each day, we removed 10 ml from each culture flask for phenotyping and replaced it with fresh media. In the first common garden we sampled

Please cite this article in press as: Ghedini and Marshall, Metabolic evolution in response to interspecific competition in a eukaryote, Current Biology (2023), https://doi.org/10.1016/j.cub.2023.06.026

on 12 occasions (i.e, every day except on days 6, 10, 13 and 15); in the second we sampled on 13 occasions (no sampling on days 7, 13, 15).

Morphology and population growth

Each sampling day, we measured the mean cell volume (volume, μm^3), cell shape (circularity) and cell density (cells/μl) of all *Dunaliella* lineages. We assessed changes in cell shape in addition to size because the shape of a cell can mediate access to resources and is thus an important component of fitness in unicellular organisms.[46,72–75]

We used light microscopy at 400x (Olympus inverted microscope) after staining a 1mL sample of each lineage with 1% Lugol's iodine. We loaded 10 μl of each stained sample on a Neubauer counting chamber (ProSciTech, Australia) and took 20 photos equally spaced around the counting grid. We then analysed the images with ImageJ and Fiji software (version 2.0)[64] to quantify the number of cells (cells μl^{-1}) and their size (μm, length and width). Cell circularity is calculated by the Fiji software as $4 \times pi \times (area/perimeter^2)$ and ranges from 0 to 1 (perfect circle). Finally, we calculated the average cell volume for each lineage by assuming a prolate spheroid shape as recommended for this species[76] ($V = (pi/6) \times width^2 \times length$); we quantified population biovolume ($\mu m^3/\mu l$) as the product of cell density and cell size obtained for each lineage.

We used the same methodology to calculate the biovolume of the focal species and its interspecific competitors during phase 1 of the experiment. For calculations of cell volume, we treated *Amphidinium* and *Phaeodactylum* as prolate spheroids, and *Nannochloropsis* as a sphere: $V = (pi/6) \times diameter^3$.

Measuring metabolism

Each sampling day, we measured oxygen evolution rates of all lineages at 20°C using 9 × 24-channel optical fluorescence oxygen readers (PreSens Sensor Dish Reader, SDR; PreSens Precision Sensing, Germany) following established protocols.[77,78] Briefly, samples were placed in 5 mL sealed vials and randomly allocated to the top-row of each reader, which was then placed horizontally under the light source (115 ± 5 μmol photons m^{-2} s^{-1}). Sensors were calibrated with 0% and 100% air saturation before the experiment. Net photosynthesis (oxygen production) was measured for 20 minutes, followed by 1 hour in the dark to measure respiration rates. Thirteen blanks were filled with media with no algal cells (obtained by centrifuging samples at 2,500 rpm for 10 min to separate the algae from the supernatant) to correct for background microbial activity since cultures were not axenic. Prior to measurements, each respirometry vial was spiked with 50 μl of sodium bicarbonate stock for a final concentration of 2 mM sodium bicarbonate to avoid carbon limitation.

The change in percentage oxygen saturation was calculated with linear regressions using the LoLinR package.[79] The rate of photosynthesis or respiration of the whole sample (VO_2; units μmol O_2/min) was then measured as $VO_2 = 1 \times ((m_a - m_b)/100 \times V\beta O_2)$ following,[80] where m_a is the rate of change of O_2 saturation in each sample (min^{-1}), m_b is the mean O_2 saturation across all blanks (min^{-1}), V is the sample volume (0.005 L) and $V\beta O_2$ is the oxygen capacity of air-saturated seawater at 20°C and 35 ppt salinity (225 μmol O_2/L). The first three minutes of measurements in the light were discarded for all samples. Respiration rates were calculated after 15 minutes of dark when oxygen levels started to show a linear decline. Finally, we converted photosynthesis and respiration rates (μmol O_2/min) to calorific energy (J/min), using the conversion factor of 0.512 J/μmol O_2 to estimate energy production and energy consumption, respectively.[81]

QUANTIFICATION AND STATISTICAL ANALYSIS

All statistical analyses were done on the data collected during the common garden tests (not during the experimental evolution phase) to assess evolved differences rather than plastic responses. We analysed data collected at 35 generations and 70 generations separately. All analyses and plots were done in RStudio (version 4.1.3), using the main packages nlme,[65] lme4,[66] car,[67] plyr[68] for analyses, and ggplot2[69] and cowplot[70] for plotting.

Changes in morphology

We assessed differences in cell morphology (size and shape) between lineages evolved with no competitors ($n = 20$), intra- ($n = 20$) or inter-specific competitors ($n = 6$ after 35 generations, $n = 10$ after 70 generations). Since cell size changed within treatments as populations grew during common garden experiments, we used a repeated measure analysis combining data between sampling days (12 and 13 sampling days for the common garden at 35 and 70 generations, respectively). Thus, we used linear mixed models that included competition treatment (3 levels) and time (experiment day) as categorical predictors, and lineage identity as random intercept to account for repeated measures; time was considered categorical because the relationship with cell morphology was non-linear. We take day 3, during the exponential growth phase, as a reference to report post hoc results on differences in cell size and shape in the main text, and we report post hoc results for each day in supplements.

Changes in metabolism

We used repeated measure analyses to test how the history of competition affected the relationship between oxygen evolution rates and biovolume at the population-level. For this analysis, we combined data from all sampling days for each common garden, starting from day 2 (i.e. the day after inoculation). Both after 35 and 70 generations of experimental evolution, oxygen rates increased linearly with biovolume during the exponential growth phase (up to day 6 included), but this correlation broke down as cultures approached

Please cite this article in press as: Ghedini and Marshall, Metabolic evolution in response to interspecific competition in a eukaryote, Current Biology (2023), https://doi.org/10.1016/j.cub.2023.06.026

carrying capacity (over ~3 $\mu m^3/\mu l$; day 7 to 16) (Figure S4). Log-transformation did not result in linearity across the entire range of biovolume. Therefore, we analysed oxygen rates separately for the exponential and stationary phase.

For data obtained after 70 generations of experimental evolution, we used linear mixed models with biovolume (covariate) and competition treatment as predictors, and lineage identity as random intercept to account for repeated measures. Because variances were heterogenous for photosynthesis during the exponential growth phase, we used a generalized linear mixed model including competition-specific variances. Finally, we used the model predictions for photosynthesis and respiration to estimate the net energy production over a 24-hour period (J/day), as 14 hr of energy produced through net photosynthesis minus 10 hr of respiration.

For data collected after 35 generations of experimental evolution, we did not measure metabolic rate on one of the sampling days (we measured metabolism on 11 days, while morphology and biomass on 12) and we could not include lineage identity as a random factor in the analysis because of a singular fit error likely due to the low replication of the interspecific competition treatment ($n = 6$ lineages). Therefore, we used simple linear models with biovolume (covariate) and competition treatment as predictors. Since this model does not account for repeated measures, we report these results as a supplementary figure (Figure S1). Nonetheless, we repeated the analyses for the 70 generations data with the same, simple linear model (i.e., without lineage as random effect, results not reported here) and obtained the same results as mixed models, suggesting that oxygen rates are not strongly affected by lineage identity.

For all analyses, oxygen rates and biovolume were not transformed but biovolume ($\mu m^3\ \mu l^{-1}$) was rescaled by multiplying for 10^{-5}. Interactions between biovolume and competition were removed when $p > 0.25$, or if the interaction was not significant and the model with interaction did not perform better than the simpler model compared by AIC.

Changes in demography

We tested how evolution in different competition environments affected demography. Specifically, we tested for differences in the maximum rates of increase (r_{max}) and maximum values of cell density (K_{pop}) for each lineage, following a three-step approach (described in detail in Ghedini et al.,[78] adapted from Malerba et al.[82]). First, we fitted four growth models to each individual lineage and chose the best-fitting model among the four candidates to describe changes in the cell density (cells μl^{-1}) of each culture over time. We used AIC to determine which growth model best described the dynamics of a culture and successful convergence was ensured for all best-fitting models. The four models were: a logistic-type sinusoidal growth model with lower asymptote forced to 0 (i.e. three-parameter logistic curve), a logistic-type sinusoidal growth model with non-zero lower asymptote (i.e. four-parameter logistic curve), a Gompertz-type sinusoidal growth model (i.e. three-parameter Gompertz curve) and a modified Gompertz-type sinusoidal growth model including population decline after reaching a maximum (i.e. four-parameter Gompertz-like curve including mortality). Second, we used the best-fitting model to estimate growth parameters (i.e., r_{max} and K_{pop}) for each culture. From each nonlinear curve, we extracted the maximum predicted value of population density (K_{pop}, cells μl^{-1}). From the first derivative of the curve, we extracted the maximum rate of population increase (r_{max}, unit: day^{-1}). Third, we used an analysis of covariance to evaluate the influence of competition on each parameter, using a linear model including the initial cell density (estimated from the previous step) as a covariate and competition environment as a factor (three levels: competition-free, intra- or inter-specific competition). The estimates of K_{pop} of the first common garden had heterogeneous variances among treatments, so we used generalized least squares models (instead of linear models) including treatment-specific variance for each level of competition treatment (varIdent function in R). We then plotted the least square means and 95% confidence intervals using Tukey p-value adjustment for comparing three estimates.

Testing predictions of metabolic theory

First, we determined the scaling exponent (B) of metabolism with cell size for our evolved populations after ten weeks of evolution (~70 generations): $MR = aM^B$, where MR is metabolic rate and M is body mass (cell size in our case). For this assessment we combined the data across the three competition treatments to assess a wider range of size. We calculated the scaling of respiration and photosynthesis separately, using linear models that included cell size and experiment day as numerical predictors. Both oxygen rates and cell size were $\log_{10}$-transformed so the scaling exponent B becomes the slope of this log-log relationship. Results did not qualitatively change when we analyzed each competition treatment separately, as each of them scaled > 1 and declined over time (Table S4).

Based on these results, we then calculated the expected scaling (B) of respiration with cell size for any given day. According to metabolic theory, the cost of production is directly proportional to cell size (scales with size at 1), so demographic parameters should scale with size at[25–27]:

$$r_{max} = M^B/M^1 = M^{B-1} \quad \text{(Equation 4)}$$

$$K_{pop} = M^0/M^B = M^{-B} \quad \text{(Equation 5)}$$

$$K_{bio} = M \times K_{pop} = M \times M^{-B} = M^{1-B} \quad \text{(Equation 6)}$$

We then tested if our data followed these predictions. Since the relationship between respiration and cell size changed as populations grew more abundant, we based our predictions on two different scaling values of B: one for the exponential growth phase (days 1-5), which we used for expectations about r_{max} which is mostly determined by growth rates early on ($B_{exponential} = 1.13$); and one for the stationary phase (days 12-16) when cultures approached carrying capacity, which we used for expectations about

Please cite this article in press as: Ghedini and Marshall, Metabolic evolution in response to interspecific competition in a eukaryote, Current Biology (2023), https://doi.org/10.1016/j.cub.2023.06.026

K_{pop} and K_{bio} ($B_{stationary}$ = 0.60). To calculate these values, we first calculated the expected value of B for each day (based on the effect of size and experiment day on B); then we averaged these values over the first 5 days to calculate $B_{exponential}$ and over the last 4 days to calculate $B_{stationary}$. Based on these values of B, we expected the following scaling:

$$r_{max} = M^{B\ exponential-1} = M^{0.13} \quad \text{(Equation 7)}$$

$$K_{pop} = M^{-B\ stationary} = M^{-0.60} \quad \text{(Equation 8)}$$

$$K_{bio} = M^{1-B\ stationary} = M^{-0.40} \quad \text{(Equation 9)}$$

We compared these predictions with the scaling of each demographic parameter with cell size (calculated over the same range of days) observed from our data. We used values of r_{max} and K_{pop} obtained from the growth models of each lineage, while we estimated maximum total biomass (K_{bio}) as the product of K_{pop} and the average cell size of each lineage. Finally, we used linear models to determine the empirical scaling of each demographic parameter with cell size (both $\log_{10}$-transformed) across the focal populations, without including competition treatment in the analyses. We used the average cell size calculated over the first 5 days for r_{max} and over days 12-16 for K_{pop} and K_{bio}.